Journal of Rock Mechanics and Geotechnical Engineering 16 (2024) 5121–5134

Contents lists available at ScienceDirect

Journal of Rock Mechanics and Geotechnical Engineering

journal homepage: www.jrmge.cn

Full Length Article

Bacterial activity and cementation pattern in biostimulated MICP-treated sand-bentonite mixtures

Yu Zhang [a, b], Xiangrui Xu [a, b], Shiqi Liu [a, b], Yijie Wang [c], Juan Du [d], Ningjun Jiang [a, b, *]

[a] Institute of Geotechnical Engineering, School of Transportation, Southeast University, Nanjing, 211189, China
[b] Jiangsu Key Laboratory of Low Carbon and Sustainable Geotechnical Engineering, Nanjing, 211189, China
[c] Department of Civil and Environmental Engineering, The Hong Kong Polytechnic University, Hung Hom, Hong Kong, China
[d] College of Civil Engineering and Architecture, Hainan University, Haikou, 570228, China

ARTICLE INFO

Article history:
Received 18 March 2024
Received in revised form
3 June 2024
Accepted 15 July 2024
Available online 17 July 2024

Keywords:
Microbially induced carbonate precipitation (MICP)
Biostimulation
Sand-clay mixtures
Bacterial activity
Cementation pattern

ABSTRACT

The application of microbially induced carbonate precipitation (MICP) in clayey soils has attracted much attention, and many studies used clay as an additive to enhance microbial mineralization efficiency in sandy soils. Within the sand-clay-bacteria-calcite system, the property and content of clay play crucial roles in affecting bacterial growth and calcite formation. More important, bentonite is particularly sensitive to changes in the geochemical environment. In this study, the sand-bentonite mixtures were treated by biostimulated MICP, aiming to provide insights into the behavior of this system. The bacterial activity and cementation pattern at different bentonite contents were evaluated through a series of tests such as enrichment tests, unconfined compressive strength (UCS) tests, cementation content measurements, mercury intrusion porosimetry (MIP) tests, scanning electron microscopy (SEM) observations, and energy dispersive X-ray spectroscopy (EDS) analyses. The findings showed that the bentonite presence promoted the enrichment of indigenous ureolytic bacteria, with lower bentonite levels enhancing ureolytic activity. Macroscopic and microscopic characterization indicated that the bentonite-coating sand structure was more conducive to the formation of large-sized calcite crystals capable of cementing soil particles compared to sand-supported and bentonite-supported structures. Additionally, excessive calcium ions (Ca^{2+}) concentrations in the cementitious solution would lead to predominant calcite deposition on soil particle surfaces, contributing minimally to strength improvement.

1. Introduction

Microbial mineralization, specifically through microbially induced carbonate precipitation (MICP) technology, has become a crucial field in geotechnical research community, as evidenced by studies from DeJong et al. (2010), Jiang et al. (2022), and Fu et al. (2023). Ureolytic bacteria-based methods are preferred within various microbial mineralization approaches for their simple urea hydrolysis processes and controllable reaction dynamics. Two primary strategies, bioaugmentation and biostimulation, are employed for microbial mineralization. Bioaugmentation introduces non-native bacteria, whereas biostimulation enhances native ureolytic bacteria, with the latter being favored for its eco-friendliness and minimal ecological impact (Wang et al., 2024). The initial applications of MICP were concentrated on sandy soils, but the cementation effect was poor in clayey soils because their low permeability impeded the injection of bacterial and cementing solutions (Cardoso et al., 2018; Xiao et al., 2022a; Zhang et al., 2023). Although the application of MICP in clayed soils had made progress in recent years (Liu et al., 2021; Mukherjee et al., 2022; Xiao et al., 2022b; He et al., 2023), MICP efficiency in clayey soils is generally lower than that in sandy ones, indicating ongoing challenges (Arpajirakul et al., 2021; Tang et al., 2023).

Recent research has focused on leveraging the adhesion between bacteria and clay to boost both the bacteria fixation and the cementation level in biocemented sandy soils (Cardoso et al., 2023). This strategy treats clay as a supplement, akin to fibers (Xiao et al., 2019), industrial by-products (Zhang et al., 2020), hydrogels (Zhao

* Corresponding author. Institute of Geotechnical Engineering, School of Transportation, Southeast University, Nanjing, 211189, China.
E-mail address: jiangn@seu.edu.cn (N. Jiang).
Peer review under responsibility of Institute of Rock and Soil Mechanics, Chinese Academy of Sciences.

https://doi.org/10.1016/j.jrmge.2024.07.005

et al., 2016), and other conventional additives. In this context, the amount of clay in biocemented soils plays a pivotal role in MICP. Cardoso et al. (2023) found that incorporating modest quantities of clay, specifically 1% kaolin and 5% bentonite, promotes sustained bacterial growth and ureolytic activity. However, high clay levels can inhibit ureolytic activity, possibly due to alumina dissolution from the clay, which reduces the pH value (Sun et al., 2019; Ma et al., 2021). Optimal clay levels exist for biocemented soils, where exceeding these levels detrimentally affects bacterial function and soil mechanics. Sun et al. (2019) observed that calcite production rates improve with kaolin up to a 7.5% threshold, after which they decrease. This pattern mirrors the trend in the unconfined compressive strength (UCS) of biocemented soils relative to calcite content. Mo et al. (2021) corroborated these findings in their investigation of biocemented sand-kaolin mixtures, highlighting an ideal clay content for biocementation. Concerning shear strength, a slight clay addition, typically 3%–10%, significantly improves cohesion in biocemented sandy soils through MICP. Above this range, the beneficial effects on cohesion diminish. The influence of clay on the internal friction angle is less clear, varying with MICP treatment methods and soil characteristics (Hataf and Jamali, 2018; Feng et al., 2022). In summary, in the sand-clay-bacteria-calcite system, the dynamics of MICP are governed by two main mechanisms: the activity of bacteria and the pattern of cementation. The impact of clay on ureolytic activity is influenced by its mineral composition and structural properties, potentially offering both positive and negative outcomes. The pattern of cementation closely correlates with the clay content, with an optimum level existing for peak mineralization efficiency. Furthermore, the bacteria-clay adhesion process may modify the formation and distribution of calcite crystals, thereby influencing the soils' mechanical properties.

Moreover, identifying active clay types, such as bentonite with 2:1 mineral structure, is crucial due to their significant interactions that affect the soils' mechanical and hydraulic characteristics, shaped by the geochemical environment (Guimarães et al., 2013; Pedrotti and Tarantino, 2018). The distinction between the effects of bentonite's diffuse double layer compression in bioaugmentation and biostimulation scenarios is complex, with potential differences in calcite distribution and the enrichment of ureolytic bacteria, emphasizing the need for comprehensive studies on biostimulated MICP-treated sand-bentonite mixtures (Ma et al., 2021; Cardoso et al., 2023).

This investigation initially explored the impact of varying bentonite contents and enrichment media substrate concentrations on various bacterial activity metrics in sand-bentonite mixtures. Subsequent stages examined how bentonite content and Ca^{2+} levels influence the UCS and microstructure of biocemented sand-bentonite mixtures, with an additional focus on pore size distribution. The results of this study aim to enhance our understanding of the sand-clay-bacteria-calcite system, with a particular focus on the effects of biostimulation.

2. Materials and methods

2.1. Materials

2.1.1. Sand, bentonite, and their mixtures

In this research, we utilized sand from the Yangzi River in Nanjing, China, which underwent air-drying and was then sieved using a US No. 18 sieve (1 mm) to eliminate large gravel and twigs, as depicted in Fig. 1a. The particle size distribution (PSD) of the refined river sand is displayed in Fig. 1b. The fundamental physical and index properties of the sand are documented in Table 1, in accordance with ASTM D2487-17 (ASTM, 2017). For the study, we used natural Ca-bentonite, shown in Fig. 1a, procured from Mu-Feng Co., Ltd. in Zhenjiang, China. This bentonite's main mineral composition includes 45.3% montmorillonite, 29.5% quartz, and 24.7% feldspar, with its PSD curve illustrated in Fig. 1b. Additional properties, such as soil classification, liquid and plastic limits, and cation exchange capacity (CEC), are detailed in Table 2.

River sand was blended with varying mass percentages of Ca-bentonite to create sand-bentonite mixtures, ensuring that each sample had the same initial dry density for consistency. The limit void ratios (e_{max} and e_{min}) of this binary soil mixture first decline and then increase as the bentonite content ranges from 0 to 100%. A critical bentonite content threshold (BC_{th}) is identified, at which point the limit void ratio is minimized. This threshold categorizes the mixtures into two structural types: below BC_{th}, mixtures display a sand-supported structure with bentonite particles filling the voids between sand grains. Above BC_{th}, the mixtures become bentonite-supported, where sand particles occupy the voids in the bentonite matrix (Zuo and Baudet, 2015; Xiao et al., 2023). Fig. 2a illustrates how the e_{max} and e_{min} vary across 11 bentonite content levels, identifying a BC_{th} value of 15%. In this context, mixtures with bentonite contents of 5%, 15%, and 45% were selected to represent the two distinct structures and the threshold one. The PSDs of these mixtures are depicted in Fig. 2b. These mixtures are classified as SM, ML, and CL at $BC = 5\%$, $BC = 15\%$, and $BC = 45\%$, respectively (ASTM, 2017).

2.1.2. Enrichment and cementation solutions for biostimulation

The enrichment medium was a mixture of nutrient broth (NB) and urea, a combination that is effective in promoting the growth of indigenous ureolytic bacteria (Wang et al., 2023). The NB, sourced from Ron Reagent, contained 10 g/L peptone, 3 g/L beef extract, and 5 g/L NaCl, offering a nutrient-rich environment conducive to bacterial development with a concentration of 20 g/L. Urea acted as a selective substrate, fostering the proliferation of ureolytic bacteria. To tailor the enrichment medium for sand-bentonite mixtures, the efficiency of bacterial enrichment over a urea concentration span of 0–200 mM (1 M = 1 mol/L) (NB-0, NBU-50, NBU-100, and NBU-200) was assessed. The cementation solution was comprised of urea and calcium chloride, supplemented with NB, with urea fixed at 200 mM and NB at 0.2 g/L. To examine how varying Ca^{2+} concentrations influenced the cementation patterns during biostimulation, calcium chloride solutions were prepared at concentrations of 50 mM, 100 mM, and 200 mM.

2.2. Methods

2.2.1. Specimen preparation

For both the enrichment and UCS tests, soil specimens were created using the one-phase mixing technique. In the enrichment test, the bacterial activity was compared in pure sand versus sand-bentonite mixtures at three different structural compositions (i.e. $BC = 5\%$, $BC = 15\%$, and $BC = 45\%$). The mass of 94.2 g of air-dried soil was mixed with 0.9 pore volume (PV) of the enrichment media. This mixture was then layered into three sections and transferred into a plastic hollow cylinder, measuring 8.0 cm in height and 5.0 cm in diameter, and compacted to a final soil height of 3.0 cm, ensuring that each of the four soil samples had a dry density of 1.60 g/cm^3. The cylinder was sealed with breathable parafilm to maintain humidity. To prevent the drying and shrinkage of bentonite from impacting the bacterial enrichment process, the prepared samples were stored in a standard curing chamber set at 20 °C and 90% relative humidity.

For preparing the UCS specimens, 0.45 PV of enrichment medium and 0.45 PV of cementation solution were mixed directly with 314 g of the sand-bentonite mixtures. This mixture was then

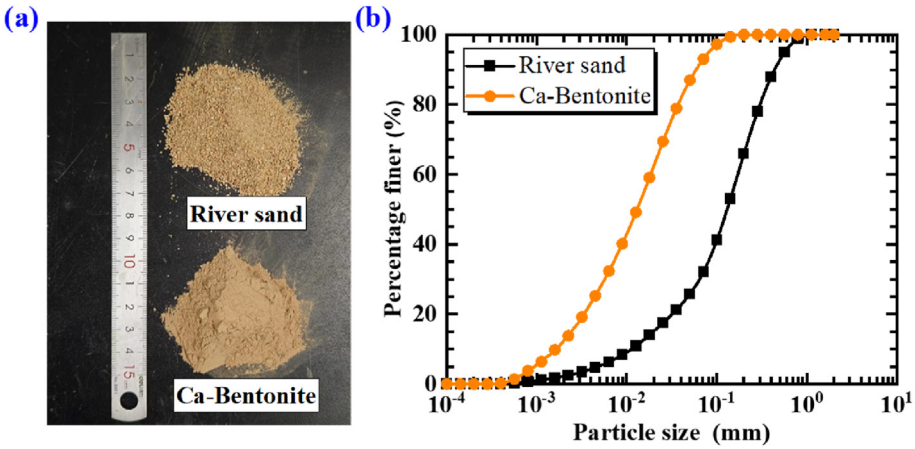

Fig. 1. (a) River sand and Ca-bentonite, and (b) particle-size distribution curves of river sand and Ca-bentonite.

Table 1
The physical and index properties of river sand.

Physical and index properties	Value
Soil classification	SM
Specific gravity, G_s	2.65
Median particle diameter, D_{50} (mm)	0.138
Coefficient of curvature, C_c	1.95
Coefficient of uniformity, C_u	14.17
Maximum void ratio, e_{max}	1.03
Minimum void ratio, e_{min}	0.55

Table 2
The properties of Ca-bentonite tested in this study.

Physical and index properties	Value
Soil classification	MH
Specific gravity, G_s	2.7
Liquid limit (%)	65.9
Plastic limit (%)	31.3
Plastic index	34.6
Cation exchange capacity (meq/100 g)	
Exchangeable Ca^{2+}	17.82
Exchangeable Mg^{2+}	5.18
Exchangeable Na^{+}	3.96
Exchangeable K^{+}	0.47
Sum	32.74

compactly layered into a detachable cylindrical plastic mold, measuring 10.0 cm in height and 5.0 cm in diameter, and sealed at the top with parafilm. The sealed mold was placed in a standard curing chamber for 7 d, ensuring a dry density of 1.60 g/cm^3 for the specimens. Additionally, untreated specimens were created without adding any calcium source, using only deionized water (DI water). The urea concentration in the enrichment media for UCS specimen preparation was determined based on the enrichment test results, to identify the most effective concentration for optimal bacterial enrichment across all samples.

2.2.2. Enrichment test

Throughout the process of enriching indigenous ureolytic bacteria, biochemical parameters including ureolytic activity, pH value, viable cell number, and concentration of urea/ammonium in the soil samples were tracked at intervals of 0 h, 12 h, 24 h, 48 h, 72 h, and 96 h. For each of these intervals, data were gathered from the central part of the soil samples. The specific methods used for these measurements are detailed in Table 3. These systematic test methods for evaluating the enrichment effect of indigenous ureolytic bacteria were verified (Wang et al., 2020, 2022b).

2.2.3. UCS test

After 7 d of biocementation, the specimens were promptly extracted from their molds for the UCS tests. This step was crucial to

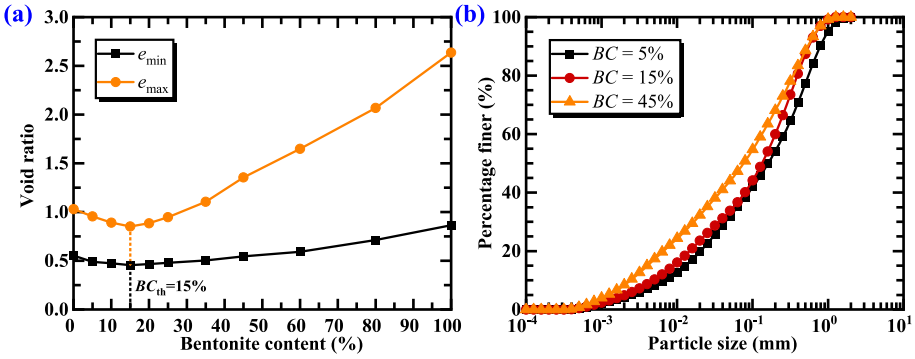

Fig. 2. (a) Limit void ratio versus bentonite content in sand-bentonite mixtures; and (b) particle size distribution curves of sand-bentonite mixtures with $BC = 5\%$, $BC = 15\%$, and $BC = 45\%$.

Table 3
Summary of biochemical characteristic measurement methods.

Parameter	Unit	Description
pH value	–	Mass of 10 g of soil sample was mixed with 20 mL of DI water and allowed to stand for 1 h. The supernatant was then tested using a pH meter (ASTM, 2019)
Ureolytic activity	mM urea min^{-1}	The electrical conductivity (EC) increment of 1 g soil sample mixed with 9 mL 1.11 M urea solution in the first 1–9 min was calculated, and then convert the volume of 1 mL of pore solution using the soil water content (Harkes et al., 2010)
Viable cell number	CFU g^{-1}	Plate counting method. The supernatant (100 μL) of soil sample mixed with DI water was taken and spread evenly onto the surface of a solid agar medium (20 g/L NB, 15 g/L agar) inside a petri dish (Wang et al., 2022b)
[Urea]	mM	Modified colorimetric urea assay method using a spectrophotometer at a wavelength of 422 nm (OD422) (Gomez et al., 2017)
$[NH_4^+]$	mM	Modified Nessler method using a spectrophotometer at a wavelength of 425 nm (OD425) (Wang et al., 2022b)

Note: CFU = colony forming units.

avoid any potential increase in strength that could result from moisture evaporation and shrinkage associated with the bentonite content. In the UCS test, specimens were subjected to axial loading at a steady rate of 1.0 mm/min. The maximum compression stress reached, or the stress at 15% strain, was recorded as the UCS, in accordance with ASTM standards (ASTM, 2016).

2.2.4. Cementation content measurement

The quantification of cementation content in biocemented sand-bentonite mixtures was performed using the hydrochloric acid dissolution method. Subsamples for this analysis were taken from the core of the specimens following the UCS tests, air-dried, and then submerged in an excess of 1.0 M HCl solution to guarantee full dissolution. After acid treatment, the samples were washed three times with DI water to remove any residual soluble substances. To avoid the loss of fine materials, such as bentonite, during the washing steps, low-speed quantitative filter paper was employed to retain these particles. Post-washing, the samples along with the filter papers were dried. The cementation content was then determined by measuring the weight of calcite relative to the sample's initial weight, expressed as a percentage. For a comprehensive explanation of the testing methods, please refer to the study of Ma et al. (2021).

2.2.5. Microstructural analysis

Mercury intrusion porosimetry (MIP) and scanning electron microscopy (SEM) were employed to study the pore size distribution and microstructure of the biocemented soil samples. For these analyses, the biocemented samples were sectioned into several 1 cm^3 cubes and subjected to freeze-drying for over 48 h. Before SEM, the samples were sputter-coated with gold to enhance the quality of the electron microscopy images. In addition, energy dispersive X-ray spectroscopy (EDS) was used in conjunction with SEM to obtain element distributions.

Table 4 gives the experimental programs for the enrichment test and UCS test, and the measurement contents for cementation content and microstructure are outlined in Table 5.

3. Testing results and data interpretation

3.1. Biochemical characteristics

3.1.1. Ureolytic activity

Ureolytic activity is a direct measurement of the impact of enrichment on native ureolytic bacteria in soils, indicating the bacteria's efficiency in breaking down urea. Fig. 3 displays the change in ureolytic activity over elapsed time in sand-bentonite mixtures with different levels of bentonite, alongside evaluating the influence of urea concentration in the enrichment media. Initially, it was found that the four original sand-bentonite mixtures were deficient in ureolytic bacteria capable of producing the urease enzyme, as shown by minimal increases in ureolytic activity in media without urea. This observation suggested that variations in ureolytic activity in the soil samples were more precisely captured in later enrichment tests using selective media with urea concentrations of 50 mM, 100 mM, and 200 mM.

Significantly, all four soil samples showed a noticeable rise in ureolytic activity after enrichment in selective media, with a pronounced increase as the urea concentration went up. The addition of bentonite seemed to fast-track the enrichment process for ureolytic bacteria. Samples containing 5%, 15%, and 45% bentonite showed enhanced ureolytic activity in just 24 h, reducing the enrichment period by half compared to the pure sand samples ($BC = 0\%$). Furthermore, the samples with a lower bentonite percentage showed superior ureolytic activity, with the $BC = 5\%$ and $BC = 15\%$ samples reaching 8.25 and 7.12 mM/min, respectively, after 96 h enrichment, in contrast to a mere 5.85 mM/ min for the pure sand samples. Nevertheless, when the bentonite content was raised to 45%, the ureolytic activity saw a decrease.

3.1.2. pH value

The pH changes during the enrichment process can essentially be divided into two stages: an initial phase characterized by acidification due to aerobic bacterial respiration and anaerobic fermentation, and a phase of alkalinization resulting from the build-up of ammonia (Wang et al., 2020). As shown in Fig. 4, the

Table 4
Experimental programs conducted in enrichment test and UCS test.

Test	Bentonite content (BC) (%)	Urea concentration in enrichment media (c_{urea}) (mM)	Ca^{2+} concentration in cementitious solution ($c_{Ca^{2+}}$) (mM)
Enrichment test	0, 5, 15, 45	0 50 100 200	–
UCS test	5, 15, 45	Selection by the enrichment test	0 50 100 200 Untreated group

Table 5
Measurement contents for cementation content and microstructure.

Measurement contents	Bentonite content (*BC*) (%)	Ca^{2+} concentration in cementitious solution (mM)
Cementation content	5, 15, 45	0 50 100 200
SEM	5, 15, 45	100 200 Untreated group
MIP	5 15 45	100 100 200 Untreated group 100
EDS	5 15 45	100 100 200 100

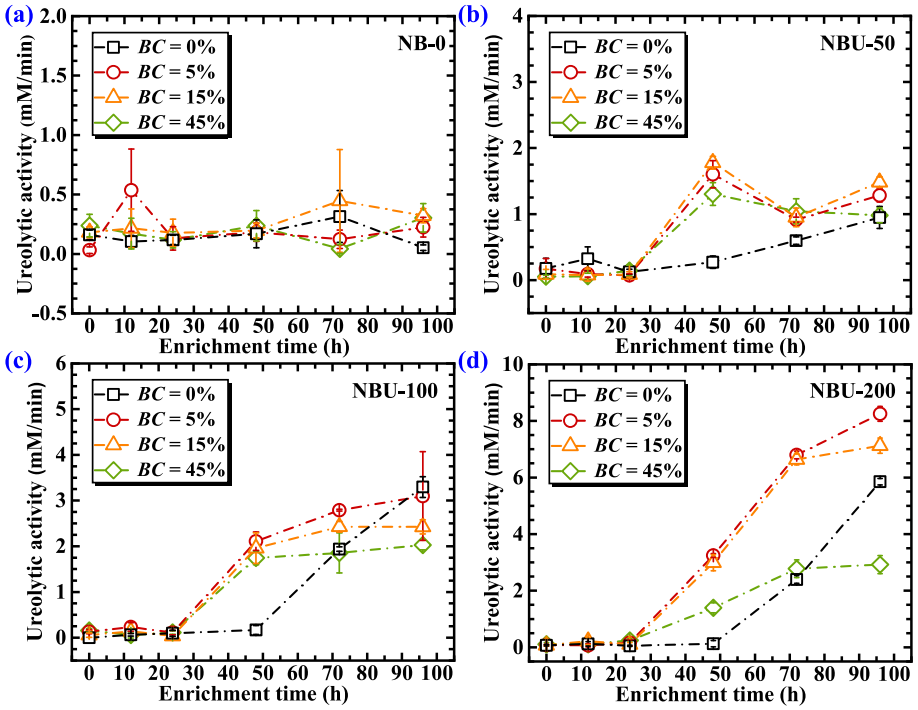

Fig. 3. Variations of ureolytic activity in sand-bentonite mixtures with enrichment time: (a) NB-0, (b) NBU-50, (c) NBU-100, and (d) NBU-200.

starting pH levels of the samples ranged from 6.94 to 7.68, but they decreased by about 0.4 in the first 24h enrichment. In the next 72 h, a gradual increase in pH was noted, attributed to the ongoing accumulation of ammonia. The data indicated that higher concentrations of urea in the selective media, specifically NBU-50, NBU-100, and NBU-200, led to more significant increases in pH values. Notably, after 96 h enrichment in NBU-200 media, the pH values are between 9.09 and 9.20, closely aligning with the theoretical ammonia equilibrium pH value of 9.3 in solution, which aids in the precipitation of calcite during MICP. Additionally, the inclusion of bentonite appeared to boost the efficiency of enriching native ureolytic bacteria, thereby hastening the pH value. Within 48 h enrichment in NBU-200 media, the pH value of the pure sand sample increased to only 8.10, whereas the bentonite-containing samples reached the pH value of 9.01–9.14.

3.1.3. Viable cell number

The count of viable cells serves as a direct indicator of the proliferation of native ureolytic bacteria in soil, with changes over time as depicted in Fig. 5. Initially, the indigenous bacteria experienced an exponential growth phase within the first 24 h across all urea concentrations in the enrichment media, with viable cell counts soaring from 10^6 CFU/g to 10^8–10^9 CFU/g. After this rapid growth phase, the number of viable cells in the NB-0 and NBU-50 media continued to increase at a steady rate. Conversely, in the NBU-100 and NBU-200 media, there was a gradual decrease in viable cell counts as enrichment time extended, notably in the NBU-200 media, where viable cell counts in all soil samples dropped to around 10^7 CFU/g by the 96-h mark.

Notably, the presence of bentonite significantly impacted bacterial proliferation. The viable cell counts in samples with 5% and

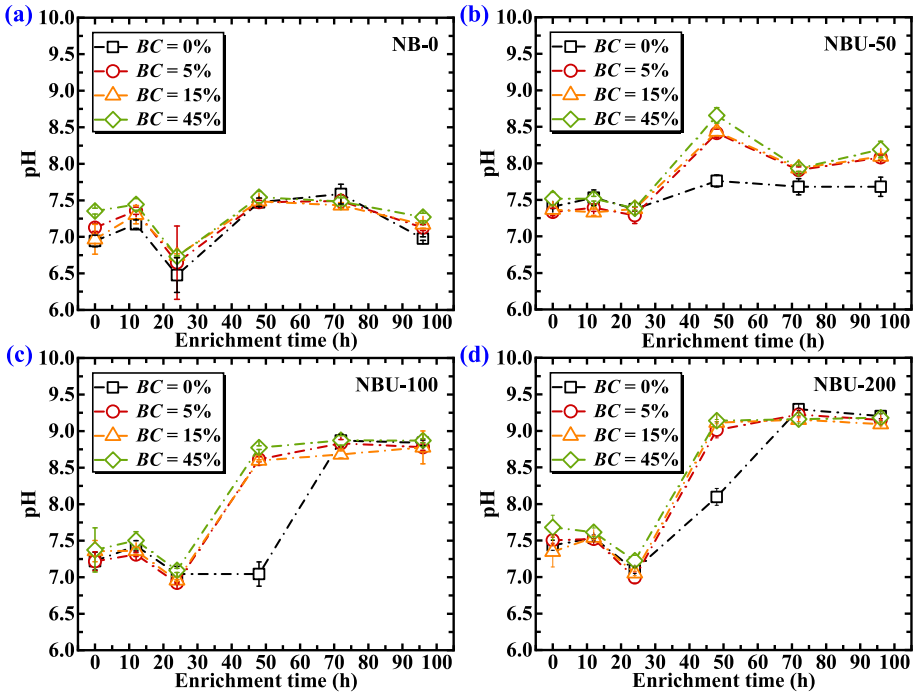

Fig. 4. Variations of pH value in sand-bentonite mixtures with enrichment time: (a) NB-0, (b) NBU-50, (c) NBU-100, and (d) NBU-200.

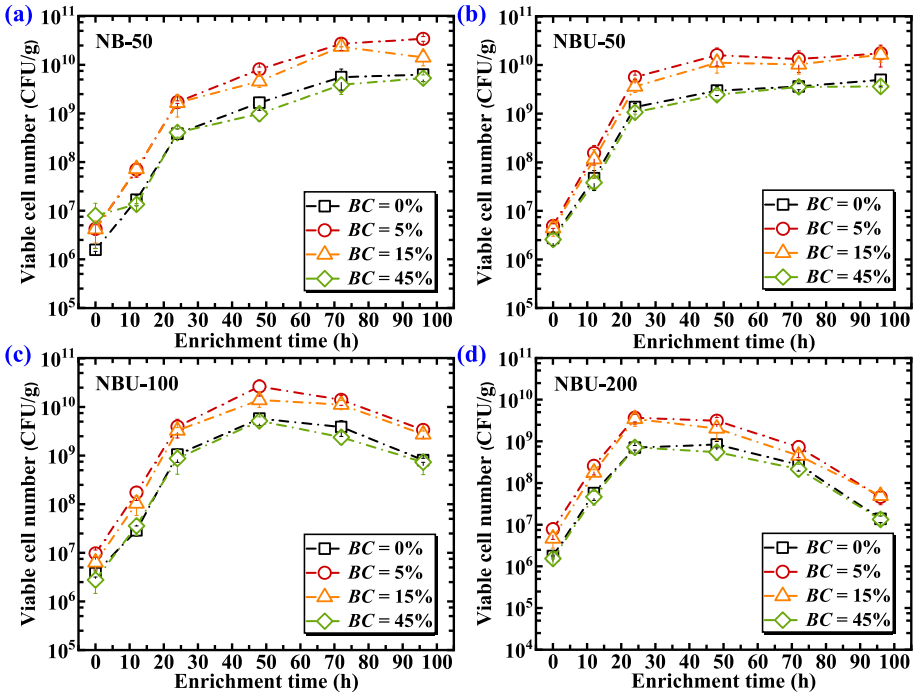

Fig. 5. Variations of viable cell number in sand-bentonite mixtures with enrichment time: (a) NB-0, (b) NBU-50, (c) NBU-100, and (d) NBU-200.

15% bentonite were consistently an order of magnitude higher than those in samples without bentonite and those with the highest bentonite content (BC = 45%). These findings underscore the importance of bacteria-clay adhesion in the enrichment process, suggesting that at optimal levels of bentonite, this adhesion can boost bacterial concentrations in the soil, thereby fostering more effective MICP.

3.1.4. Urea and ammonium concentration

The degradation rate of urea and the generation of ammonium act as indicators for the effective enrichment of native ureolytic bacteria, as well as measures of ureolytic activity. Fig. 6 illustrates a decline in urea concentration over time in all selective media, signaling that urea hydrolysis took place in the soil. By examining the curve slopes, it was observed that the rate of urea hydrolysis

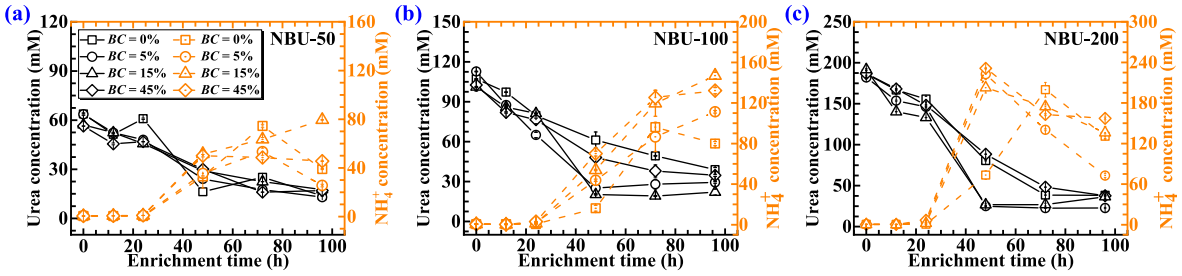

Fig. 6. Variations of urea and ammonium concentration in sand-bentonite mixtures with enrichment time: (a) NBU-50, (b) NBU-100, and (c) NBU-200.

rose with the initial concentration of urea. Simultaneously, the concentration of ammonium exhibited an upward trend. However, in alkaline conditions, some ammonium transformed into ammonia and then evaporated, leading to a discrepancy between the amounts of hydrolyzed urea and produced ammonium that fell below the theoretical 1:2 ratio, as explored by Wang et al. (2022a).

In terms of impact of bentonite on the rate of ureolysis, soils with a slight addition of bentonite showed a marked improvement in the enrichment rate of native ureolytic bacteria. This aligns with previous observations related to ureolytic activity and pH value. For example, in NBU-200 media, the urea levels in samples with 5% and 15% bentonite contents dramatically decreased from 146.26 mM and 133.14 mM to 24.95 mM and 26.70 mM, respectively, within 24–48 h enrichment. Meanwhile, samples with 0% and 45% bentonite content had higher residual urea concentrations of 60.37 mM and 80.47 mM after the same timeframe. After 48 h, urea levels in the 5% and 15% bentonite samples plateaued, while those in the 0% and 45% bentonite samples continued to decrease. A noteworthy aspect was the enhanced absorption of ammonium by bentonite, particularly when comparing the 0% and 45% bentonite samples.

3.2. UCS

From the enrichment tests, the NBU-200 media were determined to be the most effective enrichment solution for crafting biocemented samples. Using this enrichment solution, samples were prepared and cured for UCS test. Fig. 7a displays the UCS outcomes for specimens with 5%, 15%, and 45% bentonite contents treated with various Ca^{2+} concentrations. There was a discernible enhancement in the UCS of the biocemented specimens in comparison to untreated specimens after 7 d biocementation. Nevertheless, the increase in strength was modest (<50 kPa), due to the limited calcium source availability from the one-phase mixing approach. In analysis, specimens containing 5% bentonite exhibited lower strength compared to the ones containing 15% and 45% bentonite. The highest strength for specimens containing 5% bentonite was recorded at 23.30 kPa with a 100 mM Ca^{2+} treatment, whereas the ones containing 15% and 45% bentonite showed strengths over 44 kPa. This marked disparity in strength under similar conditions highlights the significant role of soil structure in the biocementation process.

To differentiate the strength gains from biocementation from the cohesive properties of clay, untreated specimens were compared as illustrated in Fig. 7b. The findings indicated that specimens containing 5% and 15% bentonite exhibited a more pronounced strength improvement, with the maximum increase reaching up to 4.84 times. On the other hand, specimens containing 45% bentonite, which had the highest bentonite content, showed only a 2.80-fold increase in strength. Where the strength of $BC = 15\%$ specimen was improved by 3.29 times under the treatment of 0 mM Ca^{2+} concentration, which may be due to the cation exchange process between NH_4^+ generated by urea hydrolysis and the interlayer Ca^{2+} in the Ca-bentonite, and the displaced Ca^{2+} form $CaCO_3$ with CO_3^{2-} in the environment. With the increase of Ca^{2+} concentration in the cementitious solution, the strength improvement showed a tendency to increase and then decrease. The $BC = 5\%$ and $BC = 15\%$ specimens reached the peak of the strength improvement under the treatment of 100 mM Ca^{2+} concentration, while the $BC = 45\%$ specimens showed a higher increase in strength with the 50 mM Ca^{2+} concentration treatment. Moreover, higher Ca^{2+} concentrations (200 mM) were found to reduce strength, especially in specimens with greater bentonite content. This reduction in strength could be linked to the diminished expansion volume of bentonite in the presence of Ca^{2+}, leading to larger pore sizes within the soil, which is less conducive to the development of calcite cementation among soil particles.

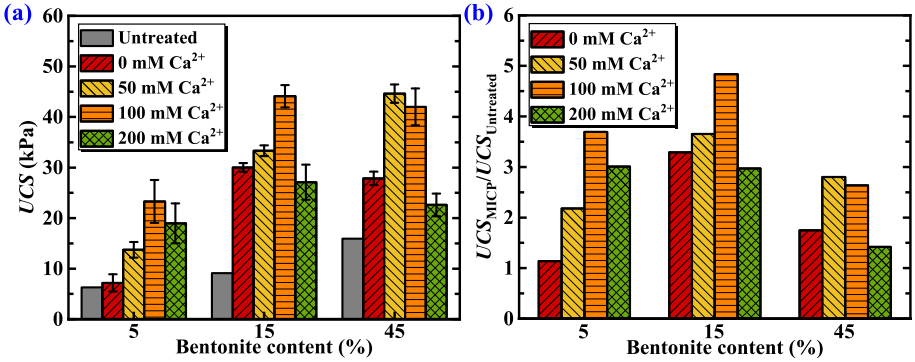

Fig. 7. UCS of biostimulated MICP-treated sand-bentonite mixtures for each condition: (a) effect of bentonite content and Ca^{2+} concentration on the strength of biocemented soils, and (b) biocementation on strength improvement in sand-bentonite mixtures.

3.3. Cementation content

Cementation content in biocemented soils is a critical measure of the MICP efficiency. As depicted in Fig. 8a, cementation content in biocemented sand-bentonite mixtures varied between 0.41% and 0.83%. Specimens with 5% and 15% bentonite showed higher cementation content compared to those with 45% bentonite, attributed to their enhanced ureolytic activity. Furthermore, an increase in Ca^{2+} concentration resulted in higher cementation content across all samples. Yet, the link between the strength gains from biocementation and the cementation content was not directly proportional. Illustrated in Fig. 8b, at Ca^{2+} concentrations below 100 mM, the strength increases with increasing cementation content. There is a correlation particularly noticeable in the samples containing 5% and 15% bentonite, which demonstrates significant strength improvements over the samples containing 45% bentonite. However, this trend of strength enhancement was significantly reduced at a Ca^{2+} concentration of 200 mM. Additionally, samples with a higher content of bentonite showed a more substantial reduction in strength. This effect was due to the complex interactions between bentonite content and Ca^{2+} concentration in biocemented soils affecting the cementation pattern, which will be explored in further microstructural analyses.

3.4. Pore size distribution

Fig. 9 shows the MIP results for specimens with 5%, 15%, and 45% bentonite contents, all of which are treated with a 100 mM Ca^{2+} concentration to evaluate their pore size distribution post-biocementation. The cumulative intrusion data against pore size highlighted that the specimens containing 15% bentonite had the lowest porosity of 31.05%, whereas the specimens containing 5% and 45% bentonite displayed marginally higher porosities of 32.44% and 31.63%, respectively. The pore size distribution for each specimen demonstrated a distinct three-peak pattern, with notable differences in the peaks across the specimens, primarily spanning from ~0.1 μm to ~300 μm. For BC = 5% bentonite samples, the pronounced peaks were found near 20 μm and 200 μm, and a smaller peak around 3 μm. The largest pores relate to voids between sand grains, and the smallest to spaces between clay particles (Cardoso et al., 2023). For BC = 15% and BC = 45% bentonite samples, the increase of bentonite content making the peak at larger pores (200 μm) was less pronounced, while peaks at smaller sizes (3–4 μm) became more evident. The presence of peaks at 7–20 μm for all three samples may reflect the interplay between the calcite filling the void and the reduced bentonite's expansion volume increasing the pore sizes during biocementation.

Fig. 10 examines the impact of varying Ca^{2+} concentrations on the pore size distribution characteristics of biocemented samples. Using the sample containing 15% bentonite as a reference, the porosity levels are recorded at 34.32%, 31.05%, and 29.55%, following treatment with DI water of 100 mM, and 200 mM Ca^{2+} concentrations, respectively, as depicted in Fig. 10a. This pattern suggests that calcite formation within soil voids leads to decreased porosity. Moreover, biocementation caused a significant redistribution of pore sizes, particularly reducing the peak associated with the smallest pores (~2 μm–3 μm) due to void filling by bacteria or calcite. An observed sharp rise in the peak for 10 μm pores stems from the reduction in bentonite's expansion volume during biocementation, a phenomenon that becomes more distinct at elevated Ca^{2+} concentrations (Cardoso et al., 2023).

3.5. SEM-EDS

Fig. 11 depicts the SEM imagery for three distinct soil samples subjected to various treatment processes. For the untreated samples, it was noted that the samples with bentonite contents of 5%, 15%, and 45% presented characteristics of sand-supported, bentonite-coating, and bentonite-supported structures, respectively, aligning with the experimental predictions. When exposed to 100 mM concentration of Ca^{2+}, the samples containing 5% bentonite were characterized by numerous tiny calcite crystals clustering together to bind soil particles. The samples containing 15% bentonite exhibited larger calcite crystals directly binding the soil particles. In contrast, the samples containing 45% bentonite exhibited precipitation of smaller calcite crystals on the surfaces of soil particles. These observations are further demonstrated in the SEM and EDS analyses in Fig. 12, where the EDS images display Si, Al, Ca, C and O, represented by purple, cyan, yellow, red, and blue colors, respectively. The comparative SEM-EDS analysis showed that the core elements of $CaCO_3$, Ca, C and O all correspond well to the shape and appearance in the SEM. The Si and Al elements mainly correspond to sand and bentonite, respectively. On the other hand, soils biocemented with higher Ca^{2+} levels showed a transformation in calcite deposition from binding between particles to surface precipitation, especially in samples with increased bentonite content (BC = 15% and BC = 45%). This alteration, alongside a decrease in bentonite expansion, might explain the change in binding patterns observed in biocemented sand-bentonite mixtures. The effect of Ca^{2+} concentration on calcite precipitation is further investigated in the BC = 15% samples treated with 100 mM and 200 mM Ca^{2+} concentrations, as depicted in Fig. 13. At a 100 mM Ca^{2+} level, bentonite particles were dispersing over the calcite surface (see Fig. 13a). However, with 200 mM Ca^{2+}

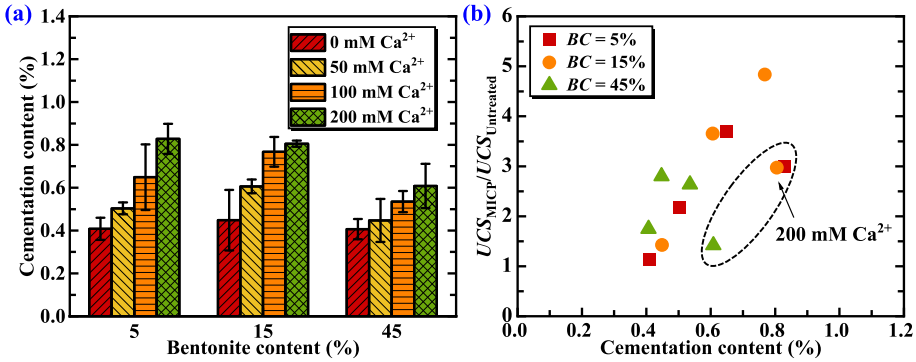

Fig. 8. Cementation content of biostimulated MICP-treated sand-bentonite mixtures. (a) Effect of bentonite content and Ca^{2+} concentration on the cementation content of biocemented soils, and (b) the relationship between the strength improvement resulting from biocementation and cementation content.

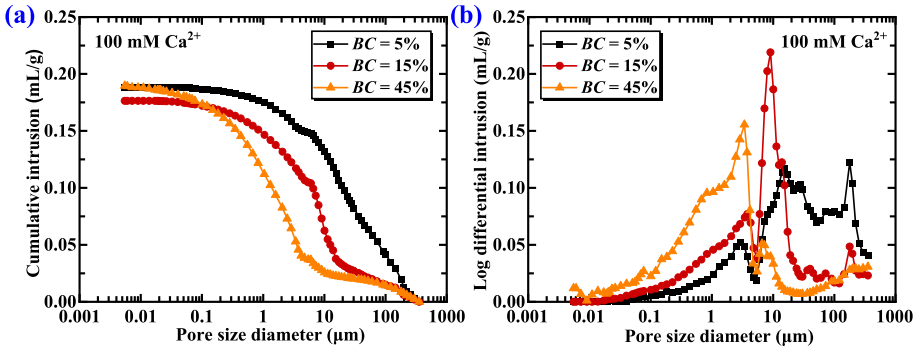

Fig. 9. Effect of bentonite content on pore size distribution in the biocemented soils: (a) Cumulative intrusion volume versus pore size diameter, and (b) differential intrusion volume versus pore size diameter.

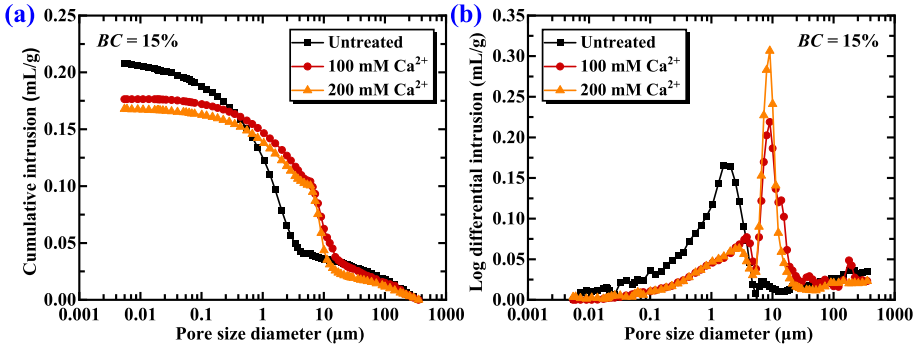

Fig. 10. Effect of treatment schemes on pore size distribution in the biocemented soils: (a) Cumulative intrusion volume versus pore size diameter, and (b) differential intrusion volume versus pore size diameter.

concentration, calcite surfaces were enveloped by aggregated bentonite particles (see Fig. 13b), a scenario which negatively affected strength enhancement.

4. Discussion

4.1. Bacterial activity in biostimulated sand-bentonite mixtures

In the method of biostimulated MICP, the crucial step is the enrichment of native ureolytic bacteria, with substrate concentration and soil characteristics playing pivotal roles in the enrichment phase. This research uncovered that the initial concentration of urea and the content of bentonite had a considerable impact on the activity of bacteria in biostimulated sand-bentonite mixtures. As illustrated by Fig. 14, there is a distinct developmental correlation between the viable cell number and ureolytic activity, which serves as a measure of bacterial functionality. When the urea concentration is low (e.g. 50 mM), the ureolytic activity remains subdued, even with a high viable cell number observed. However, with an increase in urea concentration (from 50 mM to 100–200 mM), ureolytic bacteria start to dominate the bacterial community. This shift leads to a peak in viable cell number and a significant surge in ureolytic activity. Following this phase, the accumulation of ammonium creates an alkaline environment that reduces the population of non-ureolytic bacteria, leading to a decline in overall bacterial counts. This pattern of development matches the observations of Wang et al. (2020) regarding the enrichment of ureolytic bacteria in calcareous sand. A notable distinction is noted with a higher viable cell number in the present study, which is attributed to the initial bacterial population in the soil samples and the conditions of temperature and humidity during the enrichment process.

Moreover, changes in biochemical parameters over the course of enrichment revealed that bentonite expedited the growth of ureolytic bacteria (see Fig. 3). This observation matches with that of Cardoso et al. (2023), showing that bentonite enhanced the replication of *S. pasteurii*. The primary reason for this acceleration is bentonite's provision of extra surface area for bacteria to adhere to soil particles, resulting in an increased viable cell number early in the enrichment process (Fig. 4), as noted by Cardoso et al. (2023) and Zhao et al. (2021). This leads to a quicker rise in pH values and faster urea hydrolysis (see Figs. 5 and 6). The positive effect of bentonite on bacterial growth is also linked to the creation of microenvironments within clay-bacterial clusters. The surface of montmorillonite may function as a mechanism for slow nutrient release, thereby supporting sustained bacterial growth and enhancing proliferation (Biswas et al., 2017). As depicted in Fig. 14, the quantity of viable cells in sand-bentonite mixtures surpassed those in pure sand at points of higher ureolytic activity (at viable cell number peak).

Conversely, soils with lower bentonite content (BC = 5% and 15%) showed improved ureolytic activity. This improvement is attributed not only to the increased adhesion sites offered by bentonite, but also to the interaction between the clay minerals and bacteria. The transfer of elements from clay surfaces to cell membranes via water may modify the exchangeable complex of the clay minerals. Influenced by the mineralogy of the clay and surface complexation on bacteria, this leads to the generation of reactive intermediates (radicals), enhancing ureolytic activity, as discussed by Mueller (2015) and Cardoso et al. (2023). However, Ma et al. (2021) noted that introducing bentonite into a bacterial solution could reduce ureolytic activity, possibly due to a decrease in the surrounding environment's pH caused by the Al_2O_3 in the clay

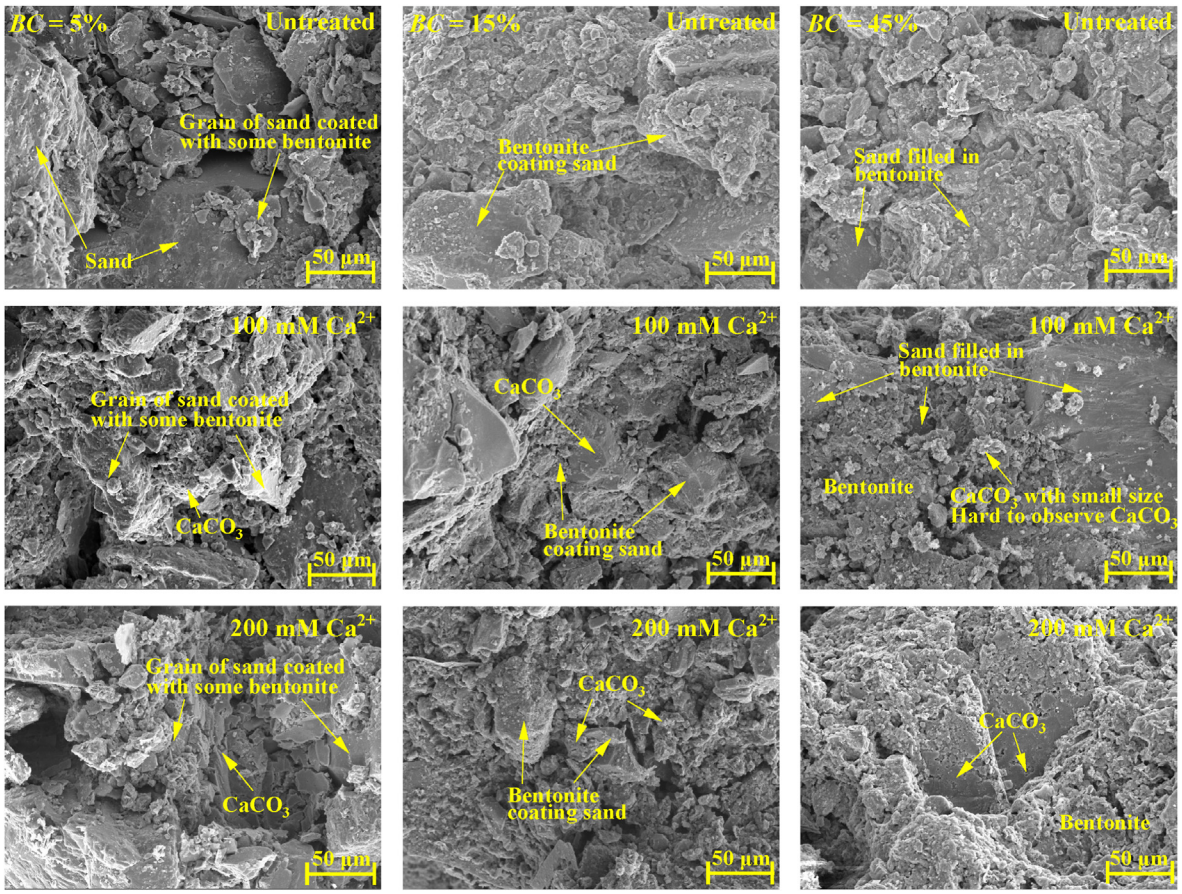

Fig. 11. SEM images of *BC* = 5% (left column), *BC* = 15% (middle column), and *BC* = 45% (right column) sand-bentonite mixtures under different treatment schemes.

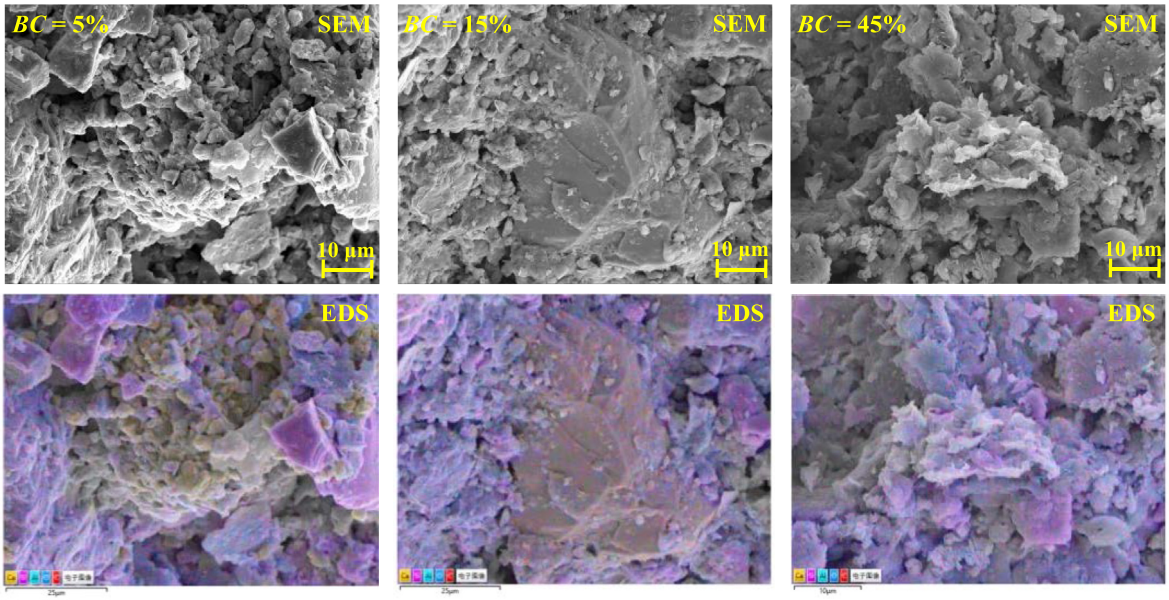

Fig. 12. SEM-EDS images of *BC* = 5% (left column), *BC* = 15% (middle column), and *BC* = 45% (right column) biocemented sand-bentonite mixtures under 100 mM Ca^{2+} concentration.

minerals (Sun et al., 2019). Despite such potential negative impacts, the enrichment of native ureolytic bacteria in sand-bentonite mixtures during the 96-h enrichment period showed no significant decrease in ureolytic activity. In soils with high bentonite content (*BC* = 45%), the reduced pore space might not support long-term bacterial viability, potentially causing an initial

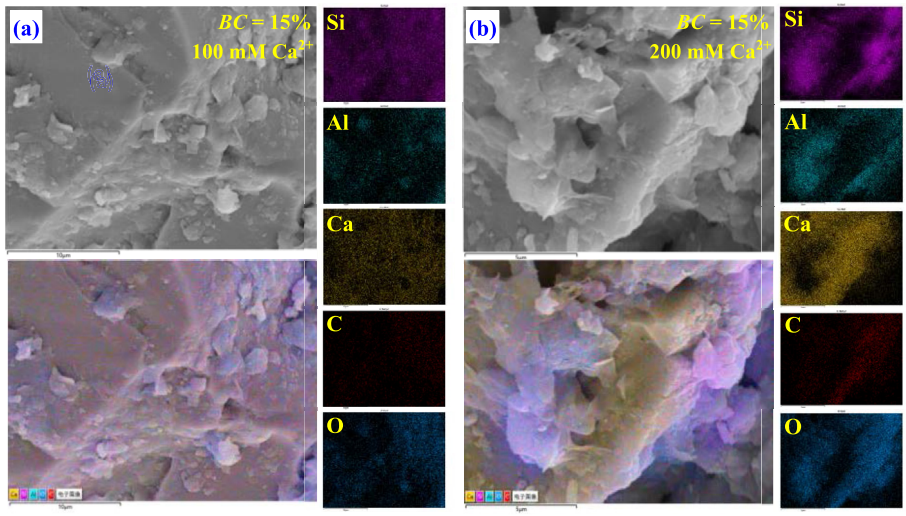

Fig. 13. EDS analysis images of calcite precipitation in biocemented sand-bentonite mixtures at different Ca^{2+} concentrations, exemplified by $BC = 15\%$ specimens: (a) 100 mM Ca^{2+}, and (b) 200 mM Ca^{2+}.

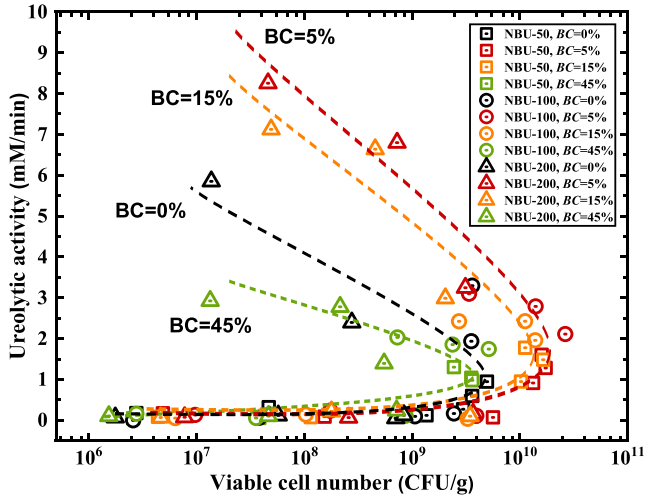

Fig. 14. The relationship between viable cell number and ureolytic activity in biostimulated sand-bentonite mixtures.

increase in ureolytic activity to fade over elapsed time, ultimately dropping below that of pure sand specimens ($BC = 0\%$).

In other words, the effects of clay particles on bacterial growth can be further summarized by combing the experimental results of this study and the research reports of other scholars in the following four aspects:

(1) The presence of clay particles can increase the adhesion sites of bacteria on soil particles, which in turn increases the viable cell number in the enrichment process;
(2) The element exchange between clay minerals and bacteria can further enhance the ureolytic activity;
(3) A smaller proportion of clay particles in the sand-clay mixtures facilitated the growth of ureolytic bacteria, and if the clay content exceeds the threshold for soil structural transformation, the smaller pore space might not support long-term bacterial viability; and
(4) In active clays such as bentonite, the surface of montmorillonite may function as a mechanism for slow nutrient release, thereby supporting sustained bacterial growth and enhancing proliferation.

4.2. Cementation pattern in biocemented sand-bentonite mixtures

In biocemented soils, calcite formation exhibits two primary patterns: the cementing of sand particles with calcite and the infilling of sand pores with calcite. The former considerably enhances the soil's mechanical strength, while the latter has a negligible effect on strength enhancement, as noted by DeJong et al. (2010) and Ma et al. (2021). Factors such as the soil's pore structure, level of saturation, grouting rate, and the mix concentration play a role in determining these patterns, as highlighted by Mujah et al. (2019) and Xiao et al. (2022a). Within biocemented sand-bentonite systems, the content of bentonite significantly influences the pattern of cementation. The findings indicate that specimens with bentonite content of 15% exhibit optimal strength improvements (Fig. 7b). This enhancement is credited to both an increase in ureolytic activity and a pore structure more conducive to calcite formation that effectively bonds the soil, as illustrated in Fig. 12 (Jiang and Soga, 2019; Sun et al., 2019).

This study employed a one-phase mixing technique for preparing specimens, where the interaction between Ca^{2+} in the cementation solution and bentonite's diffuse double layer occurred before the biostimulated MICP process. This sequence affected the distribution and formation of calcite within the altered pore structure, resulting from reduced expansion of bentonite, thereby influencing soil strength. For the specimen with 5% bentonite (sand-supported structure), decreased bentonite expansion led to larger pore sizes, which facilitated calcite crystallization on sand particles or bentonite surfaces. These crystals then aggregated into clusters, binding the sand particles together. In the 15% bentonite specimen (bentonite-coating sand), despite bentonite's reduced expansion, the small space between sand particles encouraged direct calcite bonding of the soil particles, using the bentonite-coated sand as nucleation sites, rather than forming clusters. The emergence of larger calcite crystals in this scenario significantly

enhanced soil strength (Mujah et al., 2019). For specimens with 45% bentonite (bentonite-supported structure), the extremely limited pore size resulted in calcite filling spaces in a manner akin to that observed with sand particles. A schematic representation of these cementation patterns in sand-bentonite mixtures is shown in Fig. 15.

Additionally, the interaction between Ca^{2+} concentration and bentonite influenced the cementation pattern. Fig. 8b and 11 demonstrate that at Ca^{2+} concentrations below 100 mM, the bentonite acts as nucleation sites for calcite crystal formation, significantly boosting the strength of the sand-bentonite mixtures, especially noticeable in specimens with 5% and 15% bentonite contents. Even though a few bentonite particles are presented on the calcite surface in these specimens (Fig. 13a), it hardly affects the bond strength between soil particles. Increasing Ca^{2+} concentration to 200 mM did see a rise in calcite content, but this was less effective in strengthening, particularly in higher bentonite content specimens. Research has shown that not all increases in calcite content result in stronger soils (Fujita et al., 2010; Okwadha and Li, 2010), with the key to enhancement lying in the presence of sizeable, effectively shaped calcite crystals concentrated at the soil's pore throats (Mujah et al., 2019). High Ca^{2+} levels reduced bentonite's expansion volume, creating larger pores and altering how calcite crystals were distributed over soil particles, making it challenging for calcite clusters to effectively cement the particles, particularly when calcium sources were limited. Moreover, increased supersaturation from high Ca^{2+} concentration sped up calcite nucleation, producing smaller crystals. Bentonite particles covering these smaller crystals further diminished the bonding strength (Fig. 13b), making soil void filling the primary pattern of cementation at high Ca^{2+} levels. These findings are supported by MIP test (Fig. 10) and SEM observation (Fig. 11) results.

4.3. Implications for further research and application

This study explored the dynamics of bacterial activity and the patterns of cementation in sand-bentonite mixtures treated with biostimulated MICP, offering an approach to boost the process of microbial mineralization in biocemented sands. Future research on biostimulated MICP treatment of soils suggests that incorporating a small quantity of bentonite into sand could quicken the growth of native ureolytic bacteria and increase ureolytic activity. It is vital, however, to control the bentonite ratio, ensuring that it does not surpass a critical level where the soil's structural support transitions from sand to bentonite. Only as this shift could significantly reduce the effectiveness of MICP.

Additionally, the findings from this study enrich our comprehension of the complex interactions within the sand-clay-bacteria-calcite system. Factors such as the activity state of the clay, the amount of clay presented, the composition of the enrichment medium, and the effect of Ca^{2+} on the clay's diffuse double layer are crucial considerations for enhancing the mechanical properties of biocemented soils. This is particularly relevant for specimen preparation using the one-phase mixing technique. The knowledge acquired from this study has important implications for applying biostimulated MICP more broadly, including its use in stabilizing expansive soil foundations and in developing modifications for barriers at landfill or contamination sites. It should be noted that using the one-phase mixing technique can only provide a small amount of calcium source, resulting in a low strength of the biocemented soil. Secondly, increasing the concentration of cementitious solution alone may not significantly improve the strength under the influence of Ca^{2+} compressing the diffuse double layer of bentonite. In future studies, it can be attempted to enhance the effective cementation by adjusting the composition of the enrichment media combined with increasing concentration of calcium

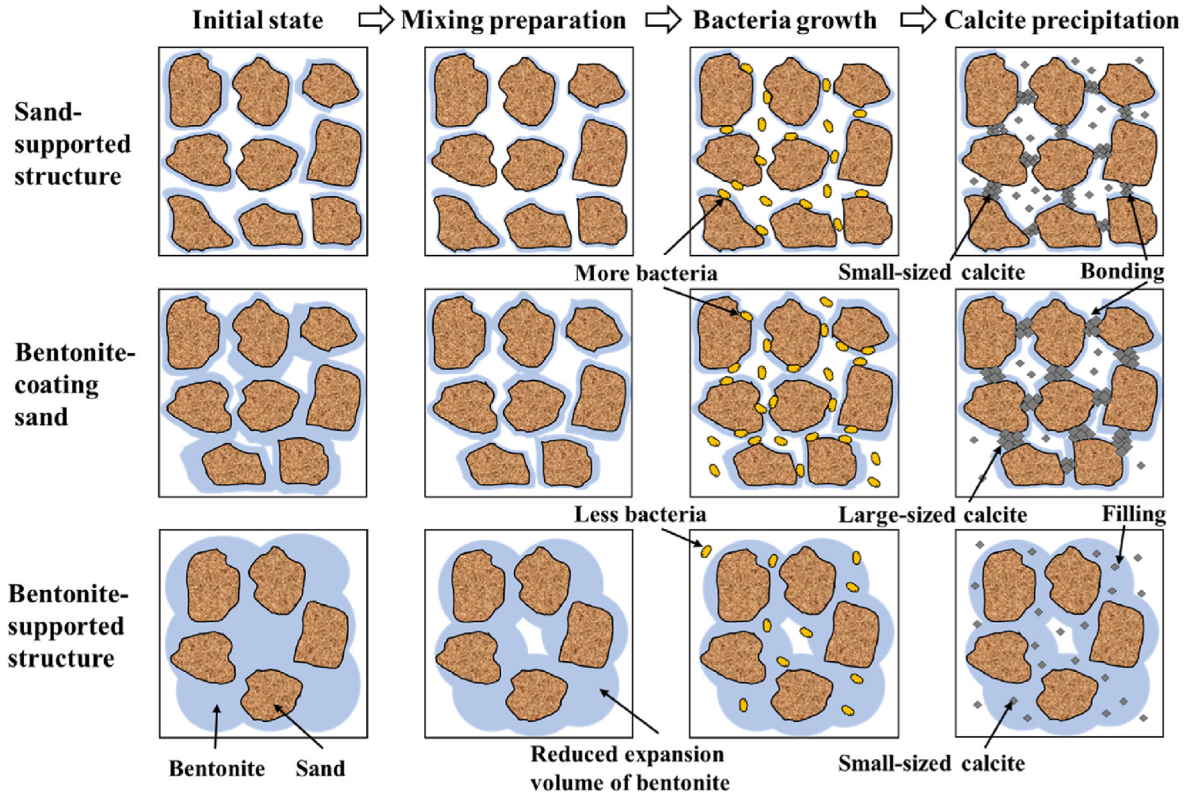

Fig. 15. The schematic diagram of the cementation pattern in biocemented sand-bentonite mixtures.

source. In addition, microfluidic chip visualization technology can also be used to reveal the evolution of cementation pattern, which in turn can provide guidance on the microscopic scale.

5. Conclusions

This research examined the effects of biostimulated MICP on sand-bentonite mixtures, and the conclusion can be drawn:

(1) The sand-bentonite mixtures demonstrated successful enrichment of native urease-producing bacteria with an initial 200 mM urea concentration in the enrichment medium. After a 96-h enrichment period, measurements of ureolytic activity, pH value, viable cell number, and concentrations of urea and ammonium aligned with the criteria for effective MICP.
(2) A smaller proportion of bentonite in the soil mixture facilitated the growth of ureolytic bacteria, which was attributed to the increased availability of bacterial adhesion sites and the creation of microenvironments conducive to clay-bacterial clusters. Moreover, the elemental exchange between bentonite and bacteria further intensified ureolytic activity.
(3) Under the condition of Ca^{2+} compressed bentonite's diffuse double layer, the bentonite-coating sand structure was more favorable for the development of large, effective calcite crystals. In contrast, sand-supported structures favored the aggregation of smaller calcite crystals into clusters. For bentonite-supported structures, calcite filled the spaces within the bentonite.
(4) At lower Ca^{2+} concentrations (below 100 mM), calcite crystals were formed around bentonite particles serving as nucleation sites, which significantly bolstered the mechanical strength of the biocemented soils. Conversely, treatment with higher Ca^{2+} concentrations resulted in calcite adherence primarily on the surface of soil particles, with bentonite particles enveloping the calcite crystals, which in turn diminished the bond strength between the soil particles.

CRediT authorship contribution statement

Yu Zhang: Writing – review & editing, Writing – original draft, Visualization, Software, Methodology, Data curation. **Xiangrui Xu:** Methodology, Investigation, Data curation. **Shiqi Liu:** Methodology, Investigation. **Yijie Wang:** Validation, Formal analysis, Conceptualization. **Juan Du:** Validation, Formal analysis. **Ningjun Jiang:** Writing – review & editing, Validation, Supervision, Resources, Project administration, Funding acquisition, Conceptualization.

Declaration of generative AI and AI-assisted technologies in the writing process

During the preparation of this work the authors used the ChatGPT in order to improve readability and language. After using this tool/service, the authors reviewed and edited the content as needed and take full responsibility for the content of the publication.

Declaration of competing interest

The authors declare that they have no known competing financial interests or personal relationships that could have appeared to influence the work reported in this paper.

Acknowledgments

This work was financially supported by the Key R&D Program Social Development Project of Jiangsu Province (Grant No. BE2023800), the Natural Science Foundation of China (Grant No. 42377166), the National Key R&D Program of China (Grant No. 2023YFC3709600).

References

Arpajirakul, S., Pungrasmi, W., Likitlersuang, S., 2021. Efficiency of microbially-induced calcite precipitation in natural clays for ground improvement. Construct. Build. Mater. 282, 122722.
ASTM D2487-17, 2017. Standard Practice for Classification of Soils for Engineered Purposes (Unified Soil Classification System). ASTM International, West Conshohocken, PA, USA.
ASTM D4972, 2019. Standard Test Methods for pH of Soils. ASTM International, West Conshohocken, PA, USA.
ASTM D2166/D2166M-13, 2016. Test Method for Unconfined Compressive Strength of Cohesive Soil. ASTM International, West Conshohocken, PA, USA.
Biswas, B., Chakraborty, A., Sarkar, B., Naidu, R., 2017. Structural changes in smectite due to interaction with a biosurfactant-producing bacterium Pseudoxanthomonas Kaohsiungensis. Appl. Clay Sci. 136, 51–57.
Cardoso, R., Pires, I., Duarte, S.O., Monteiro, G.A., 2018. Effects of clay's chemical interactions on biocementation. Appl. Clay Sci. 156, 96–103.
Cardoso, R., Borges, I., Vieira, J., Duarte, S.O., Monteiro, G.A., 2023. Interactions between clay minerals, bacteria growth and urease activity on biocementation of soils. Appl. Clay Sci. 240, 106972.
DeJong, J.T., Mortensen, B.M., Martinez, B.C., Nelson, D.C., 2010. Bio-mediated soil improvement. Ecol. Eng. 36 (2), 197–210.
Feng, D.L., Gao, H.Q., Li, Z.L., Liang, S.H., 2022. The effect of clay on the shear strength of microbially cured sand particles. Materials 15 (10), 3414.
Fu, T.Z., Saracho, A.C., Haigh, S.K., 2023. Microbially induced carbonate precipitation (MICP) for soil strengthening: a comprehensive review. Biogeotechnics 1 (1), 100002.
Fujita, Y., Taylor, J.L., Wendt, L.M., Reed, D.W., Smith, R.W., 2010. Evaluating the potential of native ureolytic microbes to remediate a 90Sr contaminated environment. Environ. Sci. Technol. 44 (19), 7652–7658.
Gomez, M.G., Anderson, C.M., Graddy, C.M., DeJong, J.T., Nelson, D.C., Ginn, T.R., 2017. Large-scale comparison of bioaugmentation and biostimulation approaches for biocementation of sands. J. Geotech. Geoenviron. Eng. 143 (5), 04016124.
Guimarães, L.D.N., Gens, A., Sánchez, M., Olivella, S., 2013. A chemo-mechanical constitutive model accounting for cation exchange in expansive clays. Geotechnique 63 (3), 221–234.
Harkes, M.P., Van Paassen, L.A., Booster, J.L., Whiffin, V.S., van Loosdrecht, M.C., 2010. Fixation and distribution of bacterial activity in sand to induce carbonate precipitation for ground reinforcement. Ecol. Eng. 36 (2), 112–117.
Hataf, N., Jamali, R., 2018. Effect of fine-grain percent on soil strength properties improved by biological method. Geomicrobiol. J. 35 (8), 695–703.
He, J., Liu, Y., Liu, L.X., Yan, B.Y., Li, L.L., Meng, H., Hang, L., Qi, Y.S., Wu, M., Gao, Y.F., 2023. Recent development on optimization of bio-cementation for soil stabilization and wind erosion control. Biogeotechnics 1 (2), 100022.
Jiang, N.J., Soga, K., 2019. Erosional behavior of gravel-sand mixtures stabilized by microbially induced calcite precipitation (MICP). Soils Found. 59 (3), 699–709.
Jiang, N.J., Wang, Y.J., Chu, J., Kawasaki, S., Tang, C.S., Cheng, L., Du, Y.J., Shashank, B.S., Singh, D.N., Han, X.L., Wang, Y.Z., 2022. Bio-mediated soil improvement: an introspection into processes, materials, characterization and applications. Soil Use Manag. 38 (1), 68–93.
Liu, B., Tang, C.S., Pan, X.H., Zhu, C., Cheng, Y.J., Xu, J.J., Shi, B., 2021. Potential drought mitigation through microbial induced calcite precipitation-MICP. Water. Resour. Res. 57 (9), e2020WR029434.
Ma, G.L., He, X., Jiang, X., Liu, H.L., Chu, J., Xiao, Y., 2021. Strength and permeability of bentonite-assisted biocemented coarse sand. Can. Geotech. J. 58 (7), 969–981.
Mo, Y.X., Yue, S.L., Zhou, Q.Z., Liu, X., 2021. Improvement and soil consistency of sand–clay mixtures treated with enzymatic-induced carbonate precipitation. Materials 14 (18), 5140.
Mueller, B., 2015. Experimental interactions between clay minerals and bacteria: a review. Pedosphere 25 (6), 799–810.
Mujah, D., Cheng, L., Shahin, M.A., 2019. Microstructural and geomechanical study on biocemented sand for optimization of MICP process. J. Mater. Civ. Eng. 31 (4), 04019025.
Mukherjee, S., Sahu, R.B., Mukherjee, J., 2022. Effect of biologically induced cementation via ureolysis in stabilization of silty soil. Geomicrobiol. J. 39 (1), 66–82.
Okwadha, G.D., Li, J., 2010. Optimum conditions for microbial carbonate precipitation. Chemosphere 81 (9), 1143–1148.
Pedrotti, M., Tarantino, A., 2018. An experimental investigation into the micromechanics of non-active clays. Geotechnique 68 (8), 666–683.
Sun, X.H., Miao, L.C., Chen, R.F., 2019. Effects of different clay's percentages on improvement of sand-clay mixtures with microbially induced calcite precipitation. Geomicrobiol. J. 36 (9), 810–818.

Tang, C.S., Pan, X.H., Cheng, Y.J., Ji, X.L., 2023. Improving hydro-mechanical behavior of loess by a bio-strategy. Biogeotechnics 1 (2), 100024.
Wang, Y.J., Han, X.L., Jiang, N.J., Wang, J., Feng, J., 2020. The effect of enrichment media on the stimulation of native ureolytic bacteria in calcareous sand. Int. J. Environ. Sci. Technol. 17 (3), 1795–1808.
Wang, Y.J., Jiang, N.J., Han, X.L., Doygun, O., Du, Y.J., 2022a. Shear behavior of bio-cemented calcareous sand treated through bio-stimulation under the direct shear condition. Bull. Eng. Geol. Environ. 81 (10), 413.
Wang, Y.J., Jiang, N.J., Han, X.L., Liu, K.W., Du, Y.J., 2022b. Biochemical, strength and erosional characteristics of coral sand treated by bio-stimulated microbial induced calcite precipitation. Acta. Geotech. 17 (9), 4217–4229.
Wang, Y.J., Jiang, N.J., Saracho, A.C., Doygun, O., Du, Y.J., Han, X.L., 2023. Compressibility characteristics of bio-cemented calcareous sand treated through the bio-stimulation approach. J. Rock Mech. Geotech. 15 (2), 510–522.
Wang, Y.J., Chen, W.B., Yin, J.H., Han, X.L., Zhang, Y., Du, Y.J., Jiang, N.J., 2024. Role of biochar in drained shear strength enhancement and ammonium removal of biostimulated MICP-treated calcareous sand. J. Geotech. Geoenviron. Eng. 150 (2), 04023140.
Xiao, Y., He, X., Evans, T.M., Stuedlein, A.W., Liu, H.L., 2019. Unconfined compressive and splitting tensile strength of basalt fiber–reinforced biocemented sand. J. Geotech. Geoenviron. Eng. 145 (9), 04019048.
Xiao, Y., He, X., Zaman, M., Ma, G.L., Zhao, C., 2022a. Review of strength improvements of biocemented soils. Int. J. GeoMech. 22 (11), 03122001.
Xiao, Y., Ma, G.L., Wu, H.R., Lu, H.L., Zaman, M., 2022b. Rainfall-induced erosion of biocemented graded slopes. Int. J. GeoMech. 22 (1), 04021256.
Xiao, Y., Fang, Q.Y., Liu, S., Shi, J.Q., Ling, Y.Y., Liu, H.L., 2023. Morphology and fines type effect on packing of binary soils. Transp. Geotech. 42, 101043.
Zhang, J.K., Su, P.D., Wen, K.J., Li, Y.D., Li, L., 2020. Mechanical performance and environmental effect of coal fly ash on MICP-induced soil improvement. KSCE. J. Civ. Eng. 24, 3189–3201.
Zhang, Y., Hu, X.L., Wang, Y.J., Jiang, N.J., 2023. A critical review of biomineralization in environmental geotechnics: applications, trends, and perspectives. Biogeotechnics 1 (1), 100003.
Zhao, Y., Zhang, P.P., Fang, H.Y., Guo, C.C., Zhang, B.B., Wang, F.M., 2021. Bentonite-assisted microbial-induced carbonate precipitation for coarse soil improvement. Bull. Eng. Geol. Environ. 80 (7), 5623–5632.
Zhao, Z., Hamdan, N., Shen, L., Nan, H.Q., Almajed, A., Kavazanjian, E., He, X.M., 2016. Biomimetic hydrogel composites for soil stabilization and contaminant mitigation. Environ. Sci. Technol. 50 (22), 12401–12410.
Zuo, L., Baudet, B.A., 2015. Determination of the transitional fines content of sand-non plastic fines mixtures. Soils Found. 55 (1), 213–219.

Dr. Ningjun Jiang is currently a Full Professor and interim Vice Director of Graduate School at Southeast University (SEU), China. He received his PhD from University of Cambridge, UK. Prior to joining SEU, he was an assistant professor at University of Hawaii at Manoa, USA. His research areas include bio-mediated geotechnics, soil remediation, and ground improvement. Prof. Jiang has published more than 80 journal and conference papers. He has received multiple research fundings from National Natural Science Foundation of China, China Ministry of Science and Technology, and Hawaii Department of Transportation, etc. He is the recipient of several academic awards, including Fredlund Award in 2019, *Acta Geotechnica* Best Paper Award in 2020, *Soils and Foundations* Editorial Board Member Award in 2021, and 75th *Géotechnique* Anniversary Early Career Award in 2023. Prof. Jiang is an Executive Deputy Editor-in-Chief for the young journal *Biogeotechnics*. Previously, he was also an editorial member of *Soils and Foundations* and *Environmental Geotechnics*.